BIOCHEMISTRY
including biophysical chemistry & molecular biology

Article

pubs.acs.org/biochemistry

Association of RrgA and RrgC into the *Streptococcus pneumoniae* Pilus by Sortases C-2 and C-3

L. El Mortaji, D. Fenel, T. Vernet, and A. M. Di Guilmi*

CEA, Institut de Biologie Structurale Jean-Pierre Ebel, Grenoble, France, CNRS, Institut de Biologie Structurale Jean-Pierre Ebel, Grenoble, France, and Université Joseph Fourier-Grenoble1, Institut de Biologie Structurale Jean-Pierre Ebel, Grenoble, France

ABSTRACT: Pili are surface-exposed virulence factors involved in the adhesion of bacteria to host cells. The human pathogen *Streptococcus pneumoniae* expresses a pilus composed of three structural proteins, RrgA, RrgB, and RrgC, and requires the action of three transpeptidase enzymes, sortases SrtC-1, SrtC-2, and SrtC-3, to covalently associate the Rrg pilins. Using a recombinant protein expression platform, we have previously shown the requirement of SrtC-1 in RrgB fiber formation and the association of RrgB with RrgC. To gain insights into the substrate specificities of the two other sortases, which remain controversial, we have exploited the same robust strategy by testing various combinations of pilins and sortases coexpressed in *Escherichia coli*. We demonstrate that SrtC-2 catalyzes the formation of both RrgA−RrgB and RrgB−RrgC complexes. The deletion and swapping of the RrgA-YPRTG and RrgB-IPQTG sorting motifs indicate that SrtC-2 preferentially recognizes RrgA and attaches it to the pilin motif lysine 183 of RrgB. Finally, SrtC-2 is also able to catalyze the multimerization of RrgA through the C-terminal D4 domains. Similar experiments have been performed with SrtC-3, which catalyzes the formation of RrgB−RrgC and RrgB−RrgA complexes. Altogether, these results provide evidence of the molecular mechanisms of association of RrgA and RrgC with the RrgB fiber shaft by SrtC-2 and SrtC-3 and lead to a revised model of the pneumococcal pilus architecture accounting for the respective contribution of each sortase.

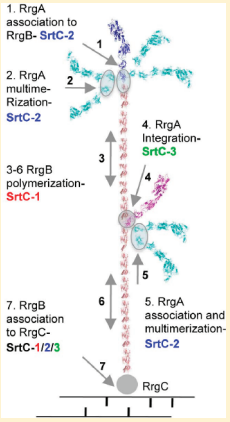

Gram-positive bacteria such as *Corynebacterium diphtheriae*, *Streptococcus pyogenes*, *Streptococcus agalactiae*, and *Streptococcus pneumoniae* harbor at their surface elongated and flexible pilus appendages, which have been shown to play important roles in host tissue colonization and pathogenesis.[1−6] These structures are formed by the polymerization of a major pilin with which minor pilins are associated. The intermolecular bonds of pili are covalent and are catalyzed by transpeptidase enzymes called sortases.[7−9]

Sortase enzymes have been classified into four groups (classes A−D) on the basis of their level of sequence identity, substrate specificity, and nature of the nucleophile acceptor.[7−10] Class A refers to the housekeeping sortases present in all Gram-positive bacteria and involved in the attachment of proteins acting as virulence factors to the cell wall peptidoglycan. Class B sortases are restricted to cell wall anchoring of heme transport proteins. Class C enzymes are pilus-associated sortases, and class D sortases play some roles in sporulation. Despite the variety of substrate recognition motifs, nucleophile acceptors, and physiological roles associated with this large family, sortases share a common enzymatic mechanism. The sortase recognition motif LPxTG-like is located near the C-terminal end of the substrate proteins and is included in the cell wall sorting signal (CWSS) region, together with a transmembrane anchor and a positively charged cytoplasmic tail. Sortases cleave the peptidic bond between the threonine and glycine residues of the LPxTG sequence, generating an intermediate acyl−enzyme complex on which the ε-amino group of a lysine residue acts as an acceptor, leading to the catalysis of an amide bond. The basis of the sortase substrate specificity and catalysis mechanism has been investigated in detail for the housekeeping sortase A of *Staphylococcus aureus* and to a lesser extent for the class B sortase IsdC (see ref 8 for a review). None of these classes of sortases are able to polymerize pilins, indicating that each sortase displays strict substrate specificity. In conclusion, the comprehensive substrate specificity of pilus-associated sortases remains to be uncovered.

Recently, crystal structures of pilus-associated sortases from *S. pneumoniae*, *S. agalactiae*, and *S. pyogenes* that allow extensive structural characterization of these sortases and renewed interpretation of sortase classification have been determined.[11−14] All sortase enzymes, including the hous-keeping sortase A, share a common catalytic triad that consists of histidine, arginine, and cysteine residues.[10] Class C enzymes, pneumococcal SrtC-1, SrtC-2, and SrtC-3, as well as GBS SrtC-1, present similar structural features; the most striking is the presence of a lid that covers the active site in a closed conformation.[11−13] The opening of this lid is required for the access of the substrate to the active site, [15] but details of this mechanism are still lacking. The *S. pyogenes* sortase Spy0129, despite being involved in pilus assembly, belongs to class B and does not present a lid covering the active site, suggesting a different substrate and acceptor motif recognition mechanism.[14]

S. pneumoniae is an important human pathogen that causes a large number of respiratory tract infections, such as pneumonia

Received: October 17, 2011
Revised: November 23, 2011
Published: November 28, 2011

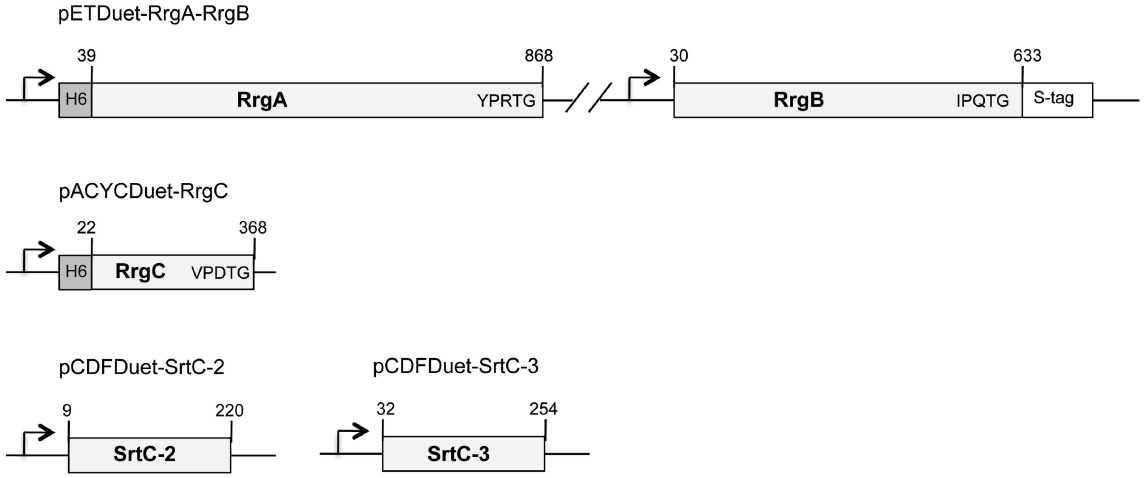

Figure 1. Schematic representation of the pETDuet−RrgA−RrgB, pACYCDuet−RrgC, pCDFDuet−SrtC-2, and pCDFDuet−SrtC-3 constructs. The arrow indicates the location of the transcription start.

and sinusitis, and also invasive diseases such as septicemia and meningitis. Among the surface-exposed virulence factors, the pneumococcal pilus plays a role in host−cell adhesion.[5,6,16] The formation of pili requires the expression of seven genes encoded by the *rlrA* pathogenicity islet, including a RofA-like transcriptional regulator (*rlrA*), three sortases (SrtC-1, SrtC-2, and SrtC-3), and three structural proteins, RrgA, RrgB, and RrgC, which harbor at their C-terminal ends sequence variations of the canonical LPxTG motif.[5] Native pili observed by electron microscopy, coupled to immunogold labeling, revealed that the pilus shaft is all along decorated by anti-RrgB antibodies, indicating that RrgB is the major pilin because its polymerization constitutes the pilus fiber.[5,16,20] On the contrary, the accessory pilins RrgA and RrgC are distributed along the fiber, in single spots or in a cluster as observed for RrgA.[5,16,20] More recently, it has been shown that RrgA and RrgC are present at the distal and proximal ends of the RrgB shaft, respectively, in accordance with the host adhesion function of RrgA with respect to fibronectin, collagen, and laminin and the putative cell wall anchoring role of RrgC.[16−19]

Sortase gene mutations in the TIGR4 strain introduced by different groups to investigate the relative contribution of the sortases in pilus formation led to a redundant role for an individual sortase. For example, polymerization of the major pilin RrgB did not rely on any three individual sortase.[18,21] Similarly, the role played by the sortases in the incorporation of the minor pilin subunits onto the RrgB backbone remains largely unresolved because no consensual overview has emerged. It had been shown that an individual *srtC-1* or *srtC-3* mutant displayed a reduced level of association of RrgA and RrgC with the pilus backbone.[20,21] In an independent study, SrtC-1 was proposed to participate in the incorporation of RrgC into the pilus,[18] but no phenotype was observed for the *srtC-3* mutant, in conflict with LeMieux's report.[20,21] Finally, no data concerning the role of SrtC-2 have been reported. One additional problem deals with the analysis of the size distribution and protein composition of the native pili, either from wild-type or mutant strains, because electrophoretic separation lacks the resolution required to provide molecular details about the pilus assembly and architecture.[5,12,18,20,21] In conclusion, because substrate specificity and catalytic molecular mechanisms are major features of pilus-associated sortases that cannot be easily addressed by the current genetic approaches, we have developed a more "constructive" approach. Using a recombinant protein expression platform, we published the first report of in vitro pneumococcal pilus assembly and established the requirement for SrtC-1 in RrgB fiber formation.[8,9,11] To gain additional insight into the molecular characterization of the three pneumococcal sortases, with regard to the substrate specificity and catalytic mechanisms, we have developed a coexpression system in *Escherichia coli*. This efficient platform allowed us to demonstrate that SrtC-1 catalyzes the transpeptidation between RrgB and RrgC, which suggests an additional role for SrtC-1 in the association of the pilus with the cell wall.[22]

In this study, we rely on the same robust strategy to analyze the specificity of the two other sortases. We show that SrtC-2 is mainly involved in the association of RrgA with the tip of the RrgB shaft, either in a monomeric or a multimeric form, while SrtC-3 inserts RrgA between RrgB subunits, all along the pilus shaft. Finally, we report that both sortases catalyze the formation of the basal RrgB−RrgC complex.

EXPERIMENTAL PROCEDURES

Cloning Procedures. The amplification of all genes was performed using the chromosomal DNA of the *S. pneumoniae* TIGR4 strain. The genes encoding RrgB (residues 30−633), RrgA (residues 39−868), RrgC (residues 22−368), SrtC-2 (residues 9−220), and SrtC-3 (residues 32−254) were cloned into pETDuet, pACYCDuet, and pCDFDuet bicistronic plasmids (Novagen), leading to constructs expressing combinations of proteins carrying histidine tags or S tags or devoid of tags (Figure 1 and Table 1). The resulting plasmids were then singly transformed or cotransformed into *E. coli* STAR (Invitrogen) to obtain strains expressing all protein combinations.

Site-Directed Mutagenesis. Mutations were introduced by polymerase chain reaction-based site-directed mutagenesis (Stratagene QuikChange II XL Site-Directed Mutagenesis Kit). Mutant plasmids were verified by DNA sequencing (Cogenics) and transformed into *E. coli* STAR for protein expression.

Coexpression and Purification of Pilin Subunits and Sortases. Bacterial cultures of Duet vectors transformed into *E. coli* STAR cells were created, and protein expression was induced in 4 mL of Terrific Broth with 0.5 mM IPTG at 37 °C over 3 h. Cells were harvested by centrifugation and chemically

Table 1. Plasmids Used in the Coexpression Experiments[a]

name	relevant characteristics
RrgA	pETDuet (AmpR), RrgA (39−868), N-terminal His tag
RrgB	pETDuet (AmpR), RrgB (30−633)
RrgC	pACYCDuet (CmR), RrgC (22−368), N-terminal His tag
SrtC-2	pCDFDuet (SmR), SrtC-2 (9−220)
RrgAB	pETDuet (AmpR), RrgA (39−868), N-terminal His tag
	pETDuet (AmpR), RrgB (30−633)
RrgAC	pETDuet (AmpR), RrgA (39−868), N-terminal His tag
	pACYCDuet (CmR), RrgC (22−368), N-terminal His tag
RrgBC	pETDuet (AmpR), RrgB (30−633)
	pACYCDuet (CmR), RrgC (22−368), N-terminal His tag
RrgA−SrtC-2	pETDuet (AmpR), RrgA (39−868), N-terminal His tag
	pCDFDuet (SmR), SrtC-2 (9−220)
RrgB−SrtC-2	pETDuet (AmpR), RrgB (30−633)
	pCDFDuet (SmR), SrtC-2 (9−220)
RrgC−SrtC-2	pACYCDuet (CmR), RrgC (22−368), N-terminal His tag
	pCDFDuet (SmR), SrtC-2 (9−220)
RrgAB−SrtC-2	pETDuet (AmpR), RrgA (39−868), N-terminal His tag
	pETDuet (AmpR), RrgB (30−633)
	pCDFDuet (SmR), SrtC-2 (9−220)
RrgAC−SrtC-2	pETDuet (AmpR), RrgA (39−868), N-terminal His tag
	pACYCDuet (CmR), RrgC (22−368), N-terminal His tag
	pCDFDuet (SmR), SrtC-2 (9−220)
RrgBC−SrtC-2	pETDuet (AmpR), RrgB (30−633)
	pACYCDuet (CmR), RrgC (22−368), N-terminal His tag
	pCDFDuet (SmR), SrtC-2 (9−220)
RrgABC−SrtC-2	pETDuet (AmpR), RrgA (39−868), N-terminal His tag
	pETDuet (AmpR), RrgB (30−633)
	pACYCDuet (CmR), RrgC (22−368), N-terminal His tag
	pCDFDuet (SmR), SrtC-2 (9−220)
RrgAB−SrtC-2$_{C179A}$	pETDuet (AmpR), RrgA (39−868), N-terminal His tag
	pETDuet (AmpR), RrgB (30−633)
	pCDFDuet (SmR), SrtC-2 (9−220), C179A mutation
RrgBC−SrtC-2$_{C179A}$	pETDuet (AmpR), RrgB (30−633)
	pACYCDuet (CmR), RrgC (22−368), N-terminal His tag
	pCDFDuet (SmR), SrtC-2 (9−220), C179A mutation
RrgABC−SrtC-2$_{C179A}$	pETDuet (AmpR), RrgA (39−868), N-terminal His tag
	pETDuet (AmpR), RrgB (30−633)
	pACYCDuet (CmR), RrgC (22−368), N-terminal His tag
	pCDFDuet (SmR), SrtC-2 (9−220), C179A mutation
RrgA$_{\Delta YPRTG}$B−SrtC-2	pETDuet (AmpR), RrgA (39−863), N-terminal His tag, deleted from the YPRTG sequence
	pETDuet (AmpR), RrgB (30−633)
	pCDFDuet (SmR), SrtC-2 (9−220)
RrgAB$_{\Delta IPQTG}$−SrtC-2	pETDuet (AmpR), RrgA (39−868), N-terminal His tag
	pETDuet (AmpR), RrgB (30−628), deleted from the IPQTG sequence
	pCDFDuet (SmR), SrtC-2 (9−220)
RrgB$_{\Delta IPQTG}$C−SrtC-2	pETDuet (AmpR), RrgB (30−628), deleted from the IPQTG sequence
	pACYCDuet (CmR), RrgC (22−368), N-terminal His tag
	pCDFDuet (SmR), SrtC-2 (9−220)
RrgBC$_{\Delta VPDTG}$−SrtC-2	pETDuet (AmpR), RrgB (30−633)
	pACYCDuet (CmR), RrgC (22−363), N-terminal His tag, deleted from the VPDTG sequence
	pCDFDuet (SmR), SrtC-2 (9−220)
RrgA$_{\Delta YPRTG::IPQTG}$B−SrtC-2	pETDuet (AmpR), RrgA (39−863), N-terminal His tag, YPRTG replaced by IPQTG
	pETDuet (AmpR), RrgB (30−633)
	pCDFDuet (SmR), SrtC-2 (9−220)
RrgA$_{\Delta YPRTG::VPDTG}$B−SrtC-2	pETDuet (AmpR), RrgA (39−863), N-terminal His tag, YPRTG replaced by VPDTG
	pETDuet (AmpR), RrgB (30−633)
	pCDFDuet (SmR), SrtC-2 (9−220)
RrgB$_{\Delta IPQTG::YPRTG}$C−SrtC-2	pETDuet (AmpR), RrgB (30−628), IPQTG replaced by YPRTG
	pACYCDuet (CmR), RrgC (22−368), N-terminal His tag
	pCDFDuet (SmR), SrtC-2 (9−220)
RrgBC$_{\Delta VPDTG::YPRTG}$−SrtC-2	pETDuet (AmpR), RrgB (30−633)
	pACYCDuet (CmR), RrgC (22−363), N-terminal His tag, VPDTG replaced by YPRTG
	pCDFDuet (SmR), SrtC-2 (9−220)
RrgAB$_{K162A}$−SrtC-2	pETDuet (AmpR), RrgA (39−868), N-terminal His tag
	pETDuet (AmpR), RrgB (30−633), K162A mutation
	pCDFDuet (SmR), SrtC-2 (9−220)
RrgAB$_{K183A}$−SrtC-2	pETDuet (AmpR), RrgA (39−868), N-terminal His tag
	pETDuet (AmpR), RrgB (30−633), K183A mutation
	pCDFDuet (SmR), SrtC-2 (9−220)
D4	pETDuet (AmpR), D4 domain of RrgA (736−859), N-terminal His tag
D4−RrgB	pETDuet (AmpR), D4 domain of RrgA (736−859), N-terminal His tag
	pETDuet (AmpR), RrgB (30−633)
D4−SrtC-2	pETDuet (AmpR), D4 domain of RrgA (736−859), N-terminal His tag
	pCDFDuet (SmR), SrtC-2 (9−220)
D4−RrgB−SrtC-2	pETDuet (AmpR), D4 domain of RrgA (736−859), N-terminal His tag
	pETDuet (AmpR), RrgB (30−633)
	pCDFDuet (SmR), SrtC-2 (9−220)
D4−RrgB−SrtC-2$_{C179A}$	pETDuet (AmpR), D4 domain of RrgA (736−859), N-terminal His tag
	pETDuet (AmpR), RrgB (30−633)
	pCDFDuet (SmR), SrtC-2 (9−220), C179A mutation
SrtC-3	pCDFDuet (SmR), SrtC-3 (32−254)
RrgA−SrtC-3	pETDuet (AmpR), RrgA (39−868), N-terminal His tag
	pCDFDuet (SmR), SrtC-3 (32−254)
RrgB-SrtC-3	pETDuet (AmpR), RrgB (30−633)

dx.doi.org/10.1021/bi201591n | *Biochemistry* 2012, 51, 342−352

Table 1. continued

name	relevant characteristics
	pCDFDuet (SmR), SrtC-3 (32−254)
RrgC−SrtC-3	pACYCDuet (CmR), RrgC (22−363), N-terminal His tag
	pCDFDuet (SmR), SrtC-3 (32−254)
RrgAB−SrtC-3	pETDuet (AmpR), RrgA (39−868), N-terminal His tag
	pETDuet (AmpR), RrgB (30−633), pCDFDuet (SmR), SrtC-3 (32−254)
RrgAC−SrtC-3	pETDuet (AmpR), RrgA (39−868), N-terminal His tag
	pACYCDuet (CmR), RrgC (22−363), N-terminal His tag
	pCDFDuet (SmR), SrtC-3 (32−254)
RrgBC−SrtC-3	pETDuet (AmpR), RrgB (30−633)
	pACYCDuet (CmR), RrgC (22−363), N-terminal His tag
	pCDFDuet (SmR), SrtC-3 (32−254)
RrgABC−SrtC-3	pETDuet (AmpR), RrgA (39−868), N-terminal His tag
	pETDuet (AmpR), RrgB (30−633)
	pACYCDuet (CmR), RrgC (22−363), N-terminal His tag
	pCDFDuet (SmR), SrtC-3 (32−254), C176A mutation
RrgAB−SrtC-3$_{C176A}$	pETDuet (AmpR), RrgA (39−868), N-terminal His tag
	pETDuet (AmpR), RrgB (30−633)
	pCDFDuet (SmR), SrtC-3 (32−254), C176A mutation
RrgBC−SrtC-3$_{C176A}$	pETDuet (AmpR), RrgB (30−633)
	pACYCDuet (CmR), RrgC (22−363), N-terminal His tag
	pCDFDuet (SmR), SrtC-3 (32−254), C176A mutation
RrgABC−SrtC-3$_{C176A}$	pETDuet (AmpR), RrgA (39−868), N-terminal His tag
	pETDuet (AmpR), RrgB (30−633)
	pACYCDuet (CmR), RrgC (22−363), N-terminal His tag
	pCDFDuet (SmR), SrtC-3 (32−254), C176A mutation

[a]The names of the constructs refer to the pilins and sortases included in each combination; the same nomenclature is employed in Figures 2−7. The names of the empty plasmids and the antibiotic resistance are indicated. For each protein, the first and last residues are given in parentheses as well as the presence of a N-terminal His tag. Point mutations, deletions, and insertions are also specified.

lysed for 20 min in 1 mL of BugBuster 1× (Novagen) diluted in 50 mM HEPES (pH 7.5), 200 mM NaCl, and 20 mM imidazole (buffer A) and supplemented with 2 μL of r-lyzozyme (Novagen) and 0.8 μL of benzonase nuclease (Novagen). The lysates were clarified by centrifugation and applied to His MultiTrap HP columns (GE Healthcare) pre-equilibrated in buffer A. Proteins were eluted in 50 mM HEPES (pH 7.5), 200 mM NaCl, and 500 mM imidazole.

Construction of TIGR4 RrgB Mutant Strains. TIGR4 (or T4) pneumococcal strains with mutations in the *rrgB* gene were generated using the Janus cassette.[23] The strains are listed in Table 2. The *rpsL1* gene was inserted into the *rpsL* locus,

Table 2. *S. pneumoniae* TIGR4 Strains

strain	relevant characteristics[a]
T4	serotype 4 TIGR4 strain
T4∇(*rpsL1*)	*Str*^{R}
T4∇(*rpsL1*)Δ(*rrgB*)∇(*kan-rpsL*)	*Kan*^{R}, *rrgB::kan-rpsL*
T4∇(*rpsL1*)Δ(*rrgB*)∇(*rrgB*)	*Str*^{R}, *rrgB*
T4∇(*rpsL1*)Δ(*rrgB*)∇(*rrgB E143A*)	*Str*^{R}, *rrgB E143A*
T4∇(*rpsL1*)Δ(*rrgB*)∇(*rrgB K162A*)	*Str*^{R}, *rrgB K162A*
T4∇(*rpsL1*)Δ(*rrgB*)∇(*rrgB K183A*)	*Str*^{R}, *rrgB K183A*

[a]Str^R, streptomycin resistance; Kan^R, kanamycin resistance.

conferring resistance to streptomycin (StrR). T4∇(*rpsL1*) displays the same phenotype as the wild-type T4 strain. The kanamycin resistance Janus cassette was amplified using primers containing upstream and downstream sequences homologous to regions flanking *rrgB*. The polymerase chain reaction product was transformed into the TIGR4 strain as previously described[24] and then plated onto Columbia blood agar plates containing kanamycin (250 μg/mL) to select for T4∇(*rpsL1*)-Δ(*rrgB*) strains. The wild-type *rrgB* gene or genes harboring the K162A and K183A point mutations were introduced via replacement of the *kan-rpsL* Janus cassette, leading to the suppression of the kanamycin resistance phenotype. The mutated gene in the mutant strain was correct as verified by sequencing.

Western Blotting. Wild-type and mutant TIGR4 strains were grown in Todd-Hewitt broth (BD) supplemented with 0.5% yeast extract (Sigma) at 37 °C in 5% CO_2, until an OD_{600} of 0.45 AU was reached. Cultures were centrifuged, and the bacterial pellet, after being washed with PBS, was treated with 200 units/mL mutanolysin (Sigma), 1 mg/mL lysozyme (Sigma), and a protease inhibitor cocktail (Complete, Roche) for 3 h at 37 °C. Cellular debris were removed by centrifugation at 11000 rpm for 15 min. Thirty microliters of each elution sample was mixed with XT Sample Buffer and XT Reducing Agent (Bio-Rad), boiled at 100 °C for 10 min, and loaded onto 4 to 12% Criterion XT Precast gels (Bio-Rad). Gels were run for approximately 3 h and subsequently electrotransferred in Trans-Blot Transfer Medium (Bio-Rad). Incubation times of 1 h were successively used for anti-RrgA polyclonal mouse antibodies (diluted 1:5000) and anti-mouse horseradish peroxidase (HRP) conjugate antibodies (Sigma, diluted 1:120000) before detection with a chemiluminescent substrate (Pierce).

Elution fractions from coexpression experiments were loaded onto the same gels, run, and subsequently electrotransferred in Trans-Blot Transfer Medium (Bio-Rad) for 30 min at 100 V. Incubation times of 1 h were successively used for the anti-RrgB, anti-SrtC-2, and anti-SrtC-3 antibody (polyclonal mouse, diluted 1:5000) and anti-mouse HRP conjugate (Sigma, diluted 1:120000) before detection with a chemiluminescent substrate (Pierce). The monoclonal anti-His antibody conjugated to HRP was diluted 1:10000.

RESULTS

SrtC-2 Catalyzes the Formation of the RrgA−RrgB and RrgB−RrgC Covalent Complexes. We have previously demonstrated the involvement of SrtC-1 in RrgB fiber formation and in the catalysis of association of RrgB with RrgC.[22] To determine the role of SrtC-2 in the association of the accessory pilins with the RrgB fiber, we have exploited the same coexpression platform.[22] Genes encoding soluble forms of

dx.doi.org/10.1021/bi201591n | Biochemistry 2012, 51, 342−352

RrgA, RrgB, RrgC, and SrtC-2, deleted from the peptide signals and the transmembrane anchors, were amplified and cloned into bicistronic vectors and the corresponding proteins coexpressed in *E. coli* (Figure 1). Proteins were purified on multiHis-Trap HP columns to which only His-tagged RrgA and RrgC, associated or not with partners, could be retained. Eluted proteins were separated by sodium dodecyl sulfate−polyacrylamide gel electrophoresis and immunoblotted with polyclonal antibodies specific for RrgB (Figure 2). The details

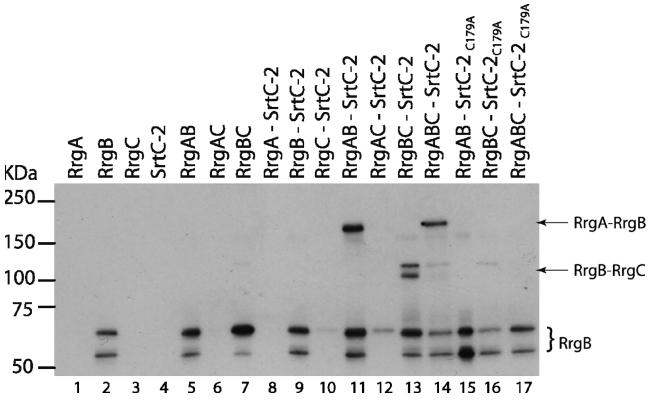

Figure 2. Formation of the RrgA−RrgB and RrgB−RrgC covalent complexes by SrtC-2. The purification of His-tagged RrgA and RrgC was performed on HisTrapTMHP columns, and the presence of RrgB in the eluted fractions was revealed with anti-RrgB polyclonal antibody. The RrgB complexes are denoted with arrows, and monomeric RrgB is denoted with a brace.

of each construct are given in Table 1. As expected, no RrgB was immunodetected in the eluted fractions of strains expressing only RrgA, RrgC, and SrtC-2 (Figure 2, lanes 1, 3, 4, 6, 8, 10, and 12). Despite the absence of a His tag on RrgB, two bands (60 and 70 kDa) are detected in the RrgB-containing eluted fractions that could be due to nonspecific binding to the His-Trap resin (Figure 2, lanes 2, 5, 7, 9, 11, and 13−17). Coexpression of RrgA, RrgB, and SrtC-2 leads to the formation of a species with an apparent molecular mass of 200 kDa, which reacts with anti-RrgB (Figure 2, lanes 11 and 14) and anti-RrgA antibodies (data not shown). This finding strongly supports the formation of a covalent link between RrgA and RrgB by SrtC-2 (calculated mass of 161 kDa). This same product is also identified when RrgC is coexpressed (Figure 2, lane 14), showing that this latter pilin subunit does not interfere with formation of the RrgA−RrgB complex. Inactivation of SrtC-2 by mutation of the catalytic Cys179 (lane 12) to Ala abolishes formation of the RrgA−RrgB complex (Figure 2, lane 15). Interestingly, two additional species of approximately 110 and 120 kDa are detected when RrgB, RrgC, and SrtC-2 are coexpressed (Figure 2, lane 13), corresponding to the RrgB−RrgC complex (calculated mass of 108 kDa). The migration of this complex as a doublet depends on the stabilization by the isopeptide bonds as shown previously.[22] Formation of the RrgB−RrgC complex is abrogated in strains lacking SrtC-2 or expressing the inactive form of the sortase (Figure 2, lanes 7 and 16). In conclusion, SrtC-2 catalyzes the covalent association of RrgB with both RrgA and RrgC.

SrtC-2 Preferentially Recognizes the RrgA-YPRTG Motif over the RrgB Sorting Sequence. To investigate in more detail the substrate specificity of SrtC-2, we deleted the cell wall sorting signals of RrgA, RrgB, and RrgC and tested the mutated pilins in the SrtC-2 coexpression system (Figure 3).

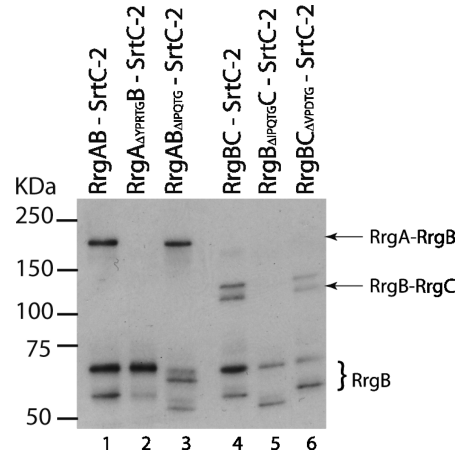

Figure 3. Substrate recognition specificity of SrtC-2. Sorting signals in RrgA, RrgB, and RrgC were deleted, and each mutant was analyzed for its ability to be recognized and processed by SrtC-2. The purification of His-tagged RrgA and RrgC was performed on HisTrapTMHP columns, and the presence of RrgB in the eluted fractions was revealed with the anti-RrgB polyclonal antibody. The RrgB complexes are denoted with arrows, and monomeric RrgB is denoted with a brace.

The details of each construct are listed in Table 1. Deletion of the RrgA-YPRTG sorting motif abrogates the formation of the RrgA−RrgB complex, while the absence of the RrgB-IPQTG motif has no effect (Figure 3, lanes 2 and 3), showing that the association of the RrgA−RrgB complex by SrtC-2 is mediated by the recognition of the YPRTG sorting motif of RrgA. On the other hand, SrtC-2 catalyzes the formation of the RrgB−RrgC complex through the initial recognition of the RrgB-IPQTG sequence (Figure 3, lanes 5 and 6). Thus, SrtC-2 presents a double substrate specificity, involving recognition of the RrgA-YPRTG motif and subsequent transpeptidation to RrgB as well as recognition of the RrgB-IPQTG motif leading to its association with RrgC.

Upon comparison of the quantities of the two complexes formed by SrtC-2 (considering that a similar amount of proteins was loaded on the polyacrylamide gels), the RrgA−RrgB complex appears to be produced to a larger extent than the RrgB−RrgC complex (Figure 2, lanes 11 and 13, and Figure 3, lanes 1 and 4). This might reflect a higher activity of SrtC-2 for the RrgA-YPRTG motif than for the RrgB-IPQTG motif. To test this hypothesis, we exchanged the sorting motifs of RrgA, RrgB, and RrgC (Figure 4A and Table 1). Replacement of the RrgA-YPRTG motif with either the IPQTG motif of RrgB or the VPDTG motif of RrgC abrogated formation of RrgA−RrgB complex by SrtC-2 (Figure 4A, lanes 2 and 3). The same approach was applied to the RrgB−RrgC complex. Replacement of the RrgB-IPQTG motif with the RrgA-YPRTG motif increased the level of the RrgB−RrgC complex formed (when compared to that of the native RrgB form), while introduction of the corresponding modifications into RrgC had no effect (Figure 4A, lanes 4−6). Thus, because the efficiency of formation of the RrgB−RrgC complex is highly increased when RrgB harbors the RrgA-YPRTG motif, it is likely that SrtC-2 is more efficient on RrgA's YPRTG motif. This observation is further supported by the detection of the covalent acyl−enzyme complex formed by SrtC-2 and RrgA

dx.doi.org/10.1021/bi201591n | *Biochemistry* 2012, 51, 342−352

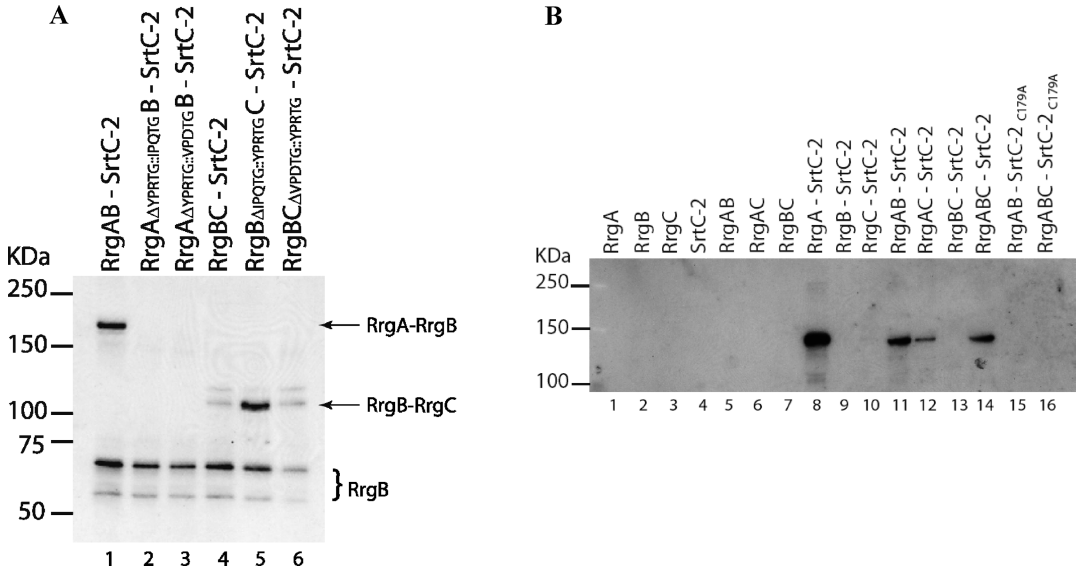

Figure 4. SrtC-2 preferentially recognized RrgA. (A) Each Rrg-LPxTG-like motif had been exchanged, and mutants were analyzed for their abilities to be recognized and processed by SrtC-2. The purification of His-tagged RrgA and RrgC was performed on HisTrapTMHP columns, and the presence of RrgB in the eluted fractions was revealed with an anti-RrgB polyclonal antibody. The RrgB complexes are denoted with arrows, and monomeric RrgB is denoted with a brace. (B) Detection of the covalent SrtC-2–RrgA acyl–enzyme complex with an anti-SrtC-2 polyclonal antibody.

(Figure 4B). The SrtC-2–RrgA complex is observed when RrgA is coexpressed with SrtC-2 (Figure 4B, lane 8; calculated mass of 120 kDa), in a manner independent of the presence of RrgB and RrgC (Figure 4B, lanes 11, 12, and 14), even though a smaller quantity of the SrtC-2–RrgA complex is detected under the latter conditions. When the catalytic Cys179 of SrtC-2 is mutated to Ala, the acyl–enzyme complex is no longer formed, indicating that this covalent association relies on the transpeptidase activity of SrtC-2 (Figure 4B, lanes 15 and 16).

SrtC-2 Catalyzes the Transpeptidation of RrgA to the RrgB Lys183 Pilin Motif. We recently determined the crystal structure of a full-length form of RrgB, which shows that the D1 domain (29–188) of one RrgB molecule interacts with the IPQTG motif of another RrgB subunit (manuscript submitted for publication). Two lysine residues within the RrgB D1 cavity, Lys162 and Lys183, are exposed, and we demonstrated that Lys183, which is part of the pilin motif, is involved in the intermolecular bond between RrgB subunits, leading to fiber polymerization. A similar observation was reported previously.[25] As RrgA and RrgB sorting signal motifs, YPRTG and IPQTG, respectively, are similar, Lys183 of RrgB might be involved in its cross-linking to RrgA. To verify this hypothesis, we mutated both Lys183 and Lys162 (used as a control) to Ala, and these RrgB mutants were tested for their ability to form a covalent complex with RrgA using the SrtC-2 coexpression system (Figure 5A and Table 1). The coexpression data show that the RrgB-Lys183Ala mutant reduces the amount of the RrgA–RrgB complex formed, while the RrgB-Lys162Ala form behaves like wild-type RrgB (Figure 5A). These data suggest that RrgA is associated with RrgB through a peptide bond catalyzed by SrtC-2 involving the RrgA-YPRTG motif and Lys183 of RrgB.

To validate, in the native pilus, the relevance of these data, we constructed a series of *S. pneumoniae* TIGR4 strain variants in which RrgB expression is suppressed by gene deletion and complemented by insertion of wild-type or mutated forms of RrgB (Glu143Ala, Lys162Ala, and Lys183Ala) (Table 2).

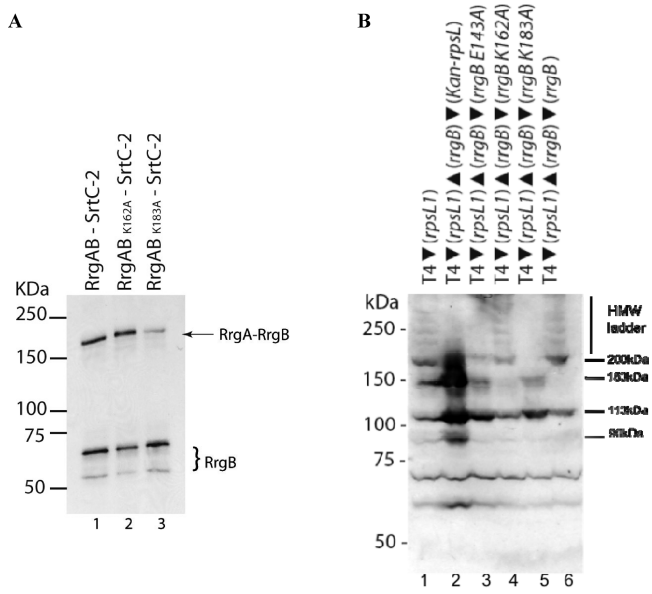

Figure 5. Intermolecular bond linking the Raga-YPRTG sequence to RrgB that involves the Lys183 pilin motif of RrgB. (A) Lys162 and Lys183 of RrgB were mutated to Ala, and the mutations were introduced into the coexpression platform. The purification of His-tagged RrgA was performed on HisTrapTMHP columns, and the presence of RrgB in the eluted fractions was revealed with an anti-RrgB polyclonal antibody. The RrgB complexes are denoted with arrows, and monomeric RrgB is denoted with a brace. (B) Glu143, Lys162, and Lys183 of RrgB were mutated to Ala, and the mutations were introduced into the native pili. Mutanolysin extracts from TIGR4 strains were loaded on 4 to 12% Criterion XT Precast gels (Bio-Rad), and Western blot analysis was performed using polyclonal rabbit antisera against RrgA. The high-molecular mass RrgA ladder monomer is denoted, as well as the proposed 90, 110, 150, and 200 kDa forms of RrgA.

Immunoblotting using an anti-RrgB serum confirmed the absence of the RrgB fiber in the *rrgB*-deleted strain and in the

dx.doi.org/10.1021/bi201591n | *Biochemistry* 2012, 51, 342–352

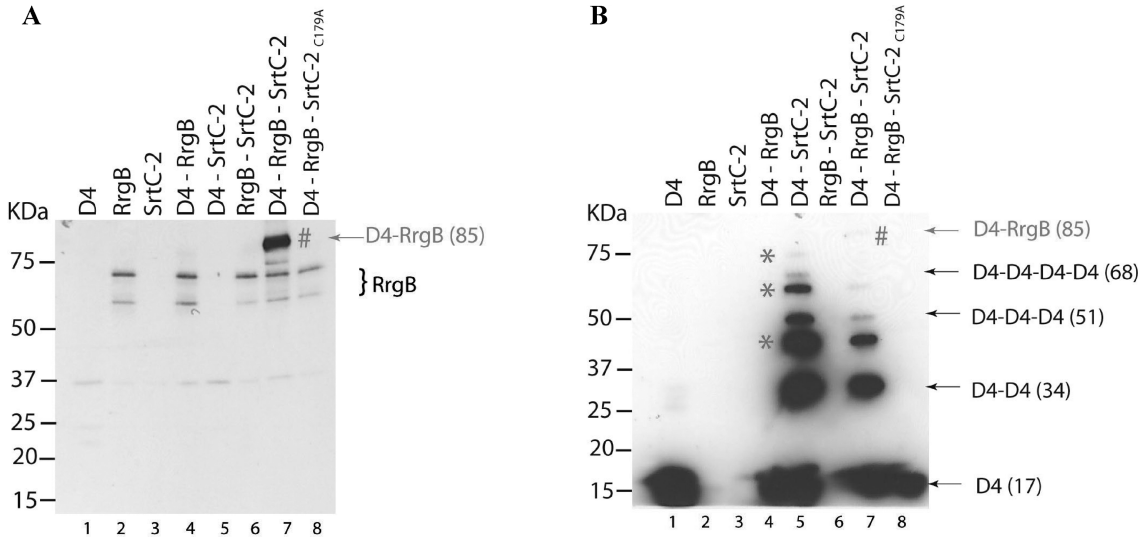

Figure 6. SrtC-2 multimerizes RrgA through association of the D4 domains. Numbers in parentheses correspond to the molecular masses of the species. The D4−RrgB complex is marked with a number sign. (A) Elution fractions immunodetected with an anti-RrgB antibody. (B) Elution fractions immunodetected with an anti-His tag HRP antibody. SrtC-2−D4 complexes are denoted with asterisks. This complex reacts against SrtC-2 antibodies (not shown).

Lys183Ala-complemented strain (data not shown). The effects of these mutations on association of RrgA with the pilus were also analyzed by Western blotting (Figure 5B). The RrgA wild-type pattern corresponds to a ladder of high-molecular mass bands, which reflects the covalent nature of the association between RrgA subunits and the size distribution of RrgB polymers (Figure 5, lanes 1 and 6). Two additional RrgA species of 110 and 200 kDa are detected.. Deletion of *rrgB* abolishes the formation of the RrgA ladder but results in the accumulation of the 110 kDa species together with a minor band migrating at 90 kDa (a likely degradation product) and of a form of RrgA around 150 kDa (Figure 5, lane 2). The association of RrgA with the RrgB fiber is fully restored once the strain is complemented with the wild-type *rrgB* gene (Figure 5, lane 6). Complementation with the Lys162Ala mutant leads to the formation of a wild-type pattern, indicating that this residue does not affect the association of RrgA with RrgB fiber (Figure 5, lane 4). Mutation of Lys183 inhibits RrgA integration, leading to the accumulation of the 110 and 150 kDa RrgA species (Figure 5, lane 5), though in smaller quantities compared with the amount of strain lacking RrgB (Figure 5, lane 2). This result suggests that Lys183, which is located within the pilin motif of the RrgB D1 domain, participates in the association of RrgA with the RrgB shaft. Interestingly, the Glu143Ala mutation, which targets the formation and stabilization of the D1 isopeptide bond in RrgB (manuscript submitted for publication), also has an effect on RrgA association, likely because of its destabilizing effect (Figure 5, lane 3). The 110 and 150 kDa RrgA species most probably correspond to monomeric forms, and the doublet migration pattern might depend on the presence of two isopeptide bonds.[26] The RrgA 200 kDa species is present only when RrgB is polymerized, suggesting that it may reflect the covalent association of RrgA with RrgB.

We have confirmed the requirement for Lys183 in RrgB polymerization because mutation of this residue totally abolishes RrgB fiber formation.[25] In this work, we observed that when RrgB harbors this mutation, no ladder form of RrgA is detected (Figure 5B, lane 5). This result could be interpreted as the inability of RrgA to be associated with the RrgB fiber because of its absence (because of the Lys183Ala mutation). However, data provided by the in vitro *E. coli* system provide another piece of evidence concerning the role of Lys183 of RrgB because it is shown that SrtC-2 recognizes this specific residue for catalyzing the RrgA transpeptidation on RrgB. In conclusion, exhaustive investigation of the molecular assembly processes of pili benefits from the combination of different approaches dealing with complementary resolution levels.

SrtC-2 Catalyzes the Multimerization of RrgA. To produce and purify a minimal RrgA−RrgB complex suitable for structural studies, we produced the isolated C-terminal D4 domain of RrgA, which was then tested for its ability to cross-link to RrgB in a sortase C-2-dependent manner. The construct engineering was based on the crystal structure of RrgA,[26] leading to the successful production in *E. coli* of a soluble form of the D4 domain (residues 736−859) (Table 1). The His-tagged RrgA−D4 construct has been introduced into the coexpression system and was shown to be associated with RrgB by the active form of SrtC-2 because a complex of ∼85 kDa, detected with anti-RrgB antibodies, is observed (Figure 6A, lane 7).

The same samples were immunodetected with an anti-His tag antibody to verify the presence of the His-tagged RrgA-D4 domain (Figure 6B). We expected to detect the following species: D4 monomers migrating at 17 kDa (in accordance with the calculated mass of 16991 Da) and the D4−RrgB complex migrating at 85 kDa (Figure 6B, lane 7, marked with a number sign). The signal intensity of the latter species is lower when detected using anti-His tag antibodies than with anti-RrgB antibodies (compare lane 7 in Figure 6A and with lane 7 in Figure 6B), because of the abundant noncomplexed His-tagged D4 eluted from the Ni column. In addition to these species, dimer (34 kDa), trimer (51 kDa), and tetramer (68 kDa) forms of D4 domains were detected when coexpressed with SrtC-2 (Figure 6B, lanes 5 and 7). These RrgA−D4 domain multimers require active SrtC-2 because only monomers are detected when coexpressed with the inactive C179A enzyme (Figure 6B, lane 8). Detection of the SrtC-2−D4 acyl−enzyme forms

dx.doi.org/10.1021/bi201591n | *Biochemistry* 2012, 51, 342−352

(Figure 6B) further supports SrtC-2-dependent RrgA−D4 multimerization as shown for full-size RrgA (Figure 4B).

The covalent RrgA−D4 dimer catalyzed by SrtC-2 has been purified to homogeneity and characterized by electrospray mass spectrometry. The expected mass of the complex of 33851.65 Da corresponds to the sum of one D4 molecule without the C-terminal GG residues (D4-YPRT) cleaved by SrtC-2 and one full-length D4 molecule (D4-YPRTGG). The presence of one isopeptide bond in each D4 domain, leading to the loss of 17 Da (one NH_3 group per bond), is also taken into consideration in the mass calculation. The D4−D4 dimer mass of 33851.85 Da corresponds to the calculated value of 33851.65 Da. The D4 monomer was also analyzed as a control; the mass of 16991.95 Da measured is again in accord with the expected mass of 16991.88 Da, which includes one isopeptide bond. The D4 domain, used as the minimal entity of the RrgA protein recognized by SrtC-2, has been used to tackle the multimerization process in place with full-length RrgA as a way to avoid the intrinsic oligomerization of RrgA when it is produced in *E. coli*.

His-tagged RrgA, coproduced with SrtC-2, was purified by Ni affinity chromatography and analyzed by gel filtration. Two populations of RrgA were detected: peak 1 corresponds to the void volume and contains high-molecular mass RrgA species, while peak 2 is composed of a unique homogeneous species of RrgA migrating at 120 kDa (data not shown). Samples from each peak were observed by negative staining transmission electron microscopy (Figure 6C). Monomeric RrgA (peak 2) appears as an elongated structure of four globules of slightly different size. This shape corresponds to the global structure of RrgA as determined by X-ray crystallography[26] and in accord with previous observations.[17] Despite the presence of some aggregates in peak 1, RrgA multimers that take the shape of a star with a nucleation center were identified (Figure 6C). These RrgA branched forms were not observed when RrgA was produced and purified in the absence of SrtC-2 (data not shown).

Roles of SrtC-3 in Pilus Biogenesis. The same coexpression system was used to investigate the function of SrtC-3 (Figure 7 and Table 1). SrtC-3 catalyzes the formation of RrgA−RrgB and RrgB−RrgC complexes when the cognate pilins are coexpressed in *E. coli* (Figure 7A, lanes 11 and 13, respectively). Both complexes are formed when all three pilins are expressed with SrtC-3 but not with the inactivated C176A SrtC-3 mutant (Figure 7A, lanes 14−17). The presence of the SrtC-3−RrgB acyl−enzyme covalent complex is detected (Figure 7A, lanes 11, 13, and 14) as it reacts with anti-SrtC-3 antibodies (not shown).

Deletions of the sorting signals were performed to identify the substrate specificity of SrtC-3 (Figure 7B). The RrgB−RrgA complex is formed through the recognition of the IPQTG motif of RrgB, because its absence impairs formation of the complex, which is not the case with the corresponding variant of RrgA (Figure 7B, lanes 1−3). With respect to the RrgB−RrgC complex, the IPQTG sequence of RrgB is processed by SrtC-3, leading to the binding of RrgB to RrgC (Figure 7B, lanes 4−6). These data indicate that SrtC-3 recognizes specifically the RrgB-IPQTG motif leading to the association of RrgB with either RrgA or RrgC.

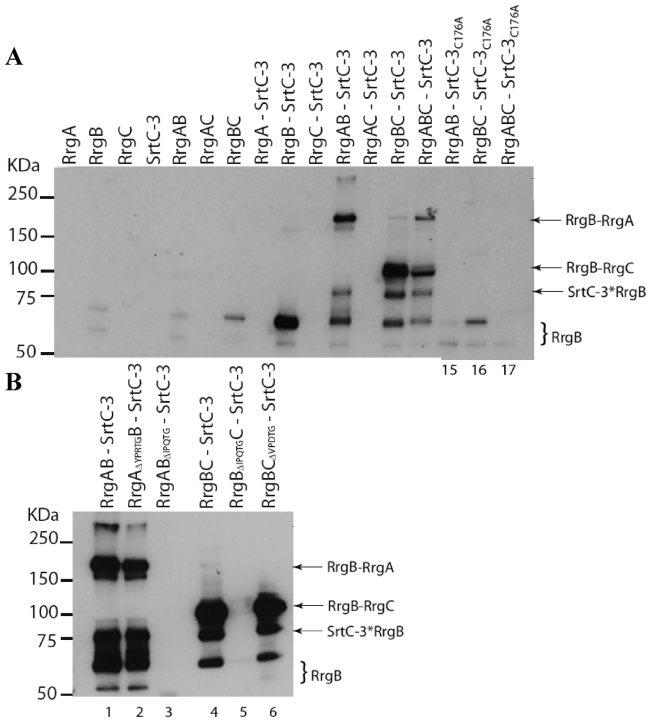

Figure 7. Covalent complexes catalyzed by SrtC-3. (A) Coexpression of RrgA, RrgB, RrgC, and SrtC-3 in *E. coli*. (B) Substrate recognition specificity of SrtC-3. Sorting signals in RrgA, RrgB, and RrgC were deleted, and each mutant was analyzed for its ability to be recognized and processed by SrtC-3. The purification of His-tagged RrgA and RrgC was performed on HisTrapTMHP columns, and the presence of RrgB in the eluted fractions was revealed with an anti-RrgB polyclonal antibody. The RrgB complexes are denoted with arrows, and monomeric RrgB is denoted with a brace.

DISCUSSION

Pili in Gram-positive bacteria are formed by the covalent association of pilins by dedicated transpeptidases. A particular feature of *S. pneumoniae* is the presence of three distinct sortases (SrtC-1, SrtC-2, and SrtC-3) encoded in the PI-1 islet, which makes understanding the role and substrate specificities of each sortase a complex task. Our understanding of the substrate specificity of all three pneumococcal sortases is still fragmentary. Reconstitution of the pilus in *E. coli* is a flexible tool for studying the behavior of multiple combinations of pilins and sortases. Indeed, the identification of the acceptor and donor proteins involved in the transpeptidation reaction catalyzed by each sortase is a prerequisite for enzymatic mechanistic studies for pilus-associated class C sortases. In this work, we established the role of SrtC-2 and SrtC-3 in pilus assembly through their contribution to the association of the minor pilins RrgA and RrgC to the RrgB fiber. Together with previous work related to the role of SrtC-1,[22] the data obtained in this work led to the revisited model of the pneumococcal pilus presented in Figure 8, which integrates for the first time the pilus architecture, the sortases mechanisms, and the putative timing of events leading to pilus assembly.

The coexpression of RrgA, RrgB, RrgC, and SrtC-2 leads to the formation of two covalent complexes, RrgA−RrgB and RrgB−RrgC. The RrgA−RrgB complex is produced in larger amounts than the RrgB−RrgC complex, the production level of the latter species being enhanced when RrgB harbors the RrgA-YPRTG sequence. Moreover, a stable covalent acyl−enzyme complex between SrtC-2 and RrgA is formed. Altogether, these data strongly suggest that RrgA is the preferred substrate for SrtC-2. We have determined the crystal structure of the

dx.doi.org/10.1021/bi201591n | *Biochemistry* 2012, 51, 342−352

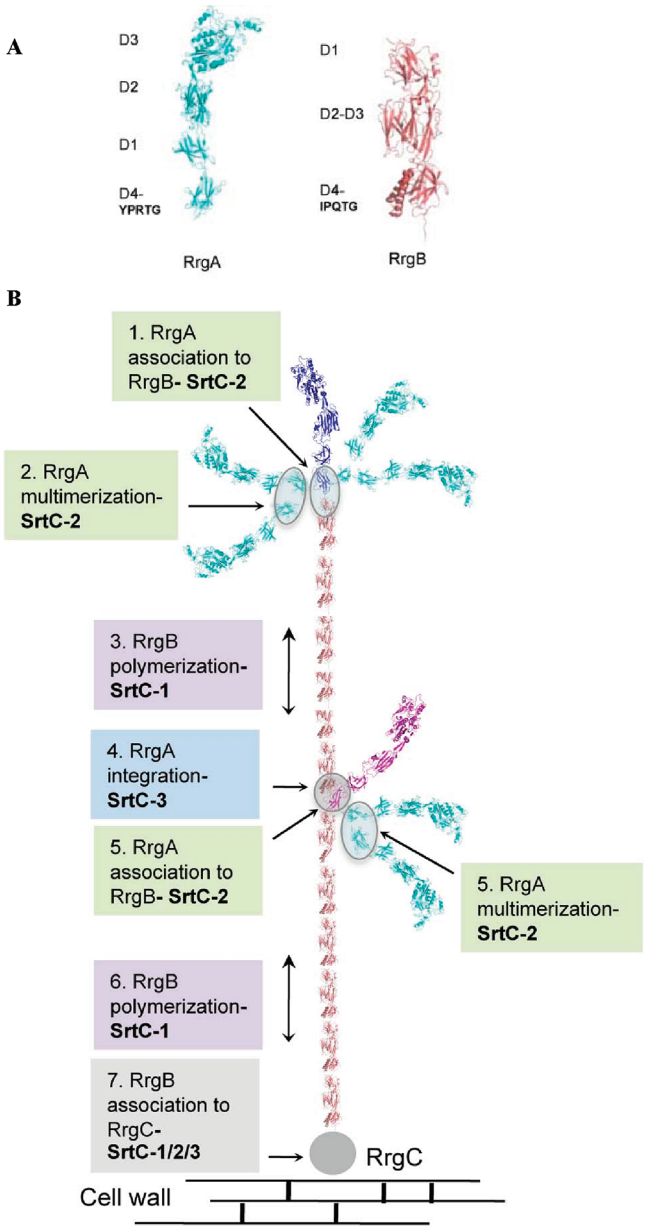

Figure 8. Pneumococcal pilus biogenesis. (A) Domain organization of RrgA and RrgB. (B) Model of pilus assembly. The function and timing of each sortase are described. SrtC-2 catalyzes step 1 of pilus assembly, the association of one RrgA molecule (violet) with the tip of the first RrgB subunit, as well as step 2, RrgA multimerization through the D4 domains (cyan). SrtC-1 is mainly involved in RrgB polymerization (steps 3 and 6), which might be interrupted by the insertion of RrgA (magenta) by the successive actions of SrtC-3 (step 4) and SrtC-2 (step 5). Finally, the anchoring of the pilus shaft to RrgC is performed by all three sortases (step 7). An unresolved question is the process of attachment of the pilus to the peptidoglycan.

full-length form of RrgB (manuscript submitted for publication). The crystal lattice generated a RrgB polymer in which the IPQTG motif of one RrgB subunit is positioned within a cavity of the D1 domain of the successive RrgB molecule. This model suggests that RrgB polymerization takes place between the IPQTG motif of one RrgB molecule and Lys183 of the pilin motif of the D1 domain from a neighboring RrgB. Because Lys183 and Lys162 are optimally positioned in the RrgB D1 domain, we wondered if these residues could also be required in the covalent association of RrgA with RrgB. Mutation of Lys183 to Ala impairs formation of the RrgA−RrgB complex, while the Lys162Ala mutation had no effect. These data have been validated in vivo, because mutation of Lys183 leads to a significant accumulation of monomeric RrgA forms. In conclusion, after recognition and cleavage of the RrgA-YPRTG sorting signal, SrtC-2 forms a peptidic bond between the C-terminal Thr and the NH_2 group of Lys183 of RrgB. Similar profiles have been observed in *S. pyogenes* pilus systems;[27,28] in the *S. pyogenes* SF370 strain, the Spy0125 adhesin subunit is linked to the major pilin Spy0128 through an intermolecular link between its C-terminal Thr723 and the amino group of Lys161 in Spy0128, which is also involved in polymerization of the major pilin.[28,29] Consequently, the association of pilus adhesin subunit Spy0125 or RrgA, in *S. pyogenes* or *S. pneumoniae*, respectively, potentially blocks further fiber extension by impeding the association of additional major pilin subunits. Because SrtC-2 catalyzes the incorporation of the adhesin RrgA at the tip of the pneumococcal pilus shaft, and considering that the pilus formation starts from the "tip", this event becomes the very first step in pilus formation.

SrtC-2 is also involved in the multimerization of RrgA through covalent linkages between the C-terminal ends of D4 domains. The identity of the acceptor lysine remains unknown despite our repeated attempts of tryptic peptide mapping using mass spectrometry. The formation and association with the fiber shaft of RrgA multimers, although not yet confirmed in the native pneumococcal pilus, can be compared to the clusters of RrgA observed by electron microscopy on purified native pili.[16] Identification of RrgA multimers in the native pneumococcal pilus is a difficult task as documented in published studies. Indeed, immunogold labeling of RrgA at the bacterial surface does not give access to individual RrgA localization.[5,16,20] On the other hand, high-level purification of native pili, despite providing localization of RrgA at the tip of the RrgB fiber, might be not representative of the whole diversity of pili structures, some of which may harbor multimerized RrgA entities.[17] This issue requires setting up electron microscopy techniques allowing labeling of single RrgA molecules in the context of the native pneumococcal pilus.

Because RrgA is considered to be the adhesin molecule of the pilus,[6,16,19,26] it may be beneficial for the bacteria to expose multiadhesin molecules to increase its binding avidity for host cell receptors. In conclusion, we propose that, as a first step in pilus formation, SrtC-2 links one RrgA molecule to one RrgB subunit (at the summit of the fiber shaft) and concomitantly associates RrgA multimers. These events are depicted in a pilus assembly model (Figure 8).

SrtC-3 catalyzes the linkage of RrgB to RrgA, through the IPQTG motif of RrgB and an unidentified lysine residue on RrgA. A possible functional justification of the formation of this covalent block by SrtC-3 would be the integration of RrgA molecules into the RrgB polymer. At some points during the RrgB polymerization catalyzed by SrtC-1, SrtC-3 might interrupt this process by overtaking the IPQTG sequence of RrgB to form a peptide bond with RrgA. SrtC-2 would be required to complete the elongation process by linking the YPRTG sequence of RrgA to the pilin lysine of RrgB. RrgA multimers may also be inserted at this step (Figure 8). SrtC-3 might also participate in the formation of the RrgB−RrgC complex via the RrgB-IPQTG peptide. Because all three sortases are able to form this complex, this building block might

be considered highly important in pilus biogenesis, most probably because it is involved in the attachement of the pilus to the peptidoglycan. The pilus assembly model we propose (Figure 8) is mainly based on biochemical data, strengthened for some of them by in vivo mutations and electron microscopy pictures. The challenge is now to validate this architecture model in the native pilus, to investigate the processes regulating pilus biogenesis, and to decipher the molecular enzymatic mechanisms of the sortases.

AUTHOR INFORMATION

Corresponding Author

*Phone: (33) (0) 4-38-78-56-34. E-mail: anne-marie.di-guilmi@ibs.fr.

Funding

This work was partly supported by EC Grant LSHM-CT-2004-512138 and ANR Grant 05-JC-JC-0049.

ACKNOWLEDGMENTS

We thank Tony Fourny for technical help and Izabel Bérard, Eric Forest, and Luca Signor from the IBS mass spectroscopy facility (LSMP, IBS). We are greatly indebted to Drs. J. P. Claverys and C. Grangeasse for providing the Janus cassette and the *R800* and *R1226* pneumococcal strains and for helpful discussions. We thank Dr. G. Schoehn, from the IBS/UVHCI platform of the Partnership for Structural Biology in Grenoble (PSB/IBS), for electron microscopy analysis.

REFERENCES

(1) Mandlik, A., Swierczynski, A., Das, A., and Ton-That, H. (2007) *Corynebacterium diphtheriae* employs specific minor pilins to target human pharyngeal epithelial cells. *Mol. Microbiol. 64*, 111−124.

(2) Abbot, E. L., Smith, W. D., Siou, G. P. S., Chiriboga, C., Smith, R. J., Wilson, J. A., Hirst, B. H., and Kehoe, M. A. (2007) Pili mediate specific adhesion of *Streptococcus pyogenes* to human tonsil and skin. *Cell. Microbiol. 9*, 1822−1833.

(3) Dramsi, S., Caliot, E., Bonne, I., Guadagnini, S., Prévost, M. C., Kojadinovic, M., Lalioui, L., Poyart, C., and Trieu-Cuot, P. (2006) Assembly and role of pile in group B streptococci. *Mol. Microbiol. 60*, 1401−1413.

(4) Konto-Ghiorghi, Y., Mairey, E., Mallet, A., Duménil, G., Caliot, E., Trieu-Cuot, P., and Dramsi, S. (2009) Dual role for pilus in adherence to epithelial cells and biofilm formation in *Streptococcus agalactiae*. *PLoS Pathog. 5*, No. e1000422.

(5) Barocchi, M. A., Ries, J., Zogaj, X., Hemsley, C., Albiger, B., Kanth, A., Dahlberg, S., Fernebro, J., Moschioni, M., Masignani, V., Hultenby, K., Taddei, A. R., Beiter, K., Wartha, F., von Euler, A., Covacci, A., Holden, D. W., Normark, S., Rappuoli, R., and Henriques-Normark, B. (2006) A pneumococcal pilus influences virulence and host inflammatory responses. *Proc. Natl. Acad. Sci. U.S.A. 103*, 2857−2862.

(6) Nelson, A. L., Ries, J., Bagnoli, F., Dahlberg, S., Falkner, S., Rounioja, S., Tschop, J., Morfeldt, E., Ferlenghi, I., Hilleringmann, M., Holden, D. W., Rappuoli, R., Normark, S., Barocchi, M. A., and Henriques-Normark, B. (2007) RrgA is a pilus-associated adhesin in *Streptococcus pneumoniae*. *Mol. Microbiol. 66*, 329−340.

(7) Dramsi, S., Magnet, S., Davison, S., and Arthur, M. (2008) Covalent attachment of proteins to peptidoglycan. *FEMS Microbiol. Rev. 32*, 307−320.

(8) Clancy, K. C., Melvin, J. A., and McCafferty, D. G. (2010) Sortase transpeptidases: Insights into mechanism, substrate specificity, and inhibition. *Biopolymers 94*, 385−396.

(9) Hendrickx, A. P., Budzik, J. M., Oh, S. Y., and Schneewind, O. (2011) Architects at the bacterial surface: Sortases and the assembly of pili with isopeptide bonds. *Nat. Rev. Microbiol. 9*, 166−176.

(10) Marraffini, L. A., Dedent, A. C., and Schneewind, O. (2006) Sortases and the art of anchoring proteins to the envelopes of Gram-positive bacteria. *Microbiol. Mol. Biol. Rev. 70*, 192−221.

(11) Manzano, C., Contreras-Martel, C., El Mortaji, L., Izoré, T., Fenel, D., Vernet, T., Schoehn, G., Di Guilmi, A. M., and Dessen, A. (2008) Sortase-mediated pilus fiber biogenesis in *Streptococcus pneumoniae*. *Structure 16* (12), 1838−1848.

(12) Neiers, F., Madhurantakam, C., Fälker, S., Manzano, C., Dessen, A., Normark, S., Henriques-Normark, B., and Achour, A. (2009) Two crystal structures of pneumococcal pilus sortase C provide novel insights into catalysis and substrate specificity. *J. Mol. Biol. 393* (3), 704−716.

(13) Cozzi, R., Malito, E., Nuccitelli, A., D'Onofrio, M., Martinelli, M., Ferlenghi, I., Grandi, G., Telford, J. L., Maione, D., and Rinaudo, D. C. (2011) Structure analysis and site-directed mutagenesis of defined key residues and motives for pilus-related sortase C1 in group B *Streptococcus*. *FASEB J. 25* (6), 1874−1886.

(14) Kang, H. J., Coulibaly, F., Proft, T., and Baker, E. N. (2011) Crystal structure of Spy0129, a *Streptococcus pyogenes* class B sortase involved in pilus assembly. *PLoS One 6*, e15969.

(15) Manzano, C., Izoré, T., Job, V., Di Guilmi, A. M., and Dessen, A. (2009) Sortase activity is controlled by a flexible lid in the pilus biogenesis mechanism of Gram-positive pathogens. *Biochemistry 48* (44), 10549−10557.

(16) Hilleringmann, M., Giusti, F., Baudner, B. C., Masignani, V., Covacci, A., Rappuoli, R., Barocchi, M. A., and Ferlenghi, I. (2008) Pneumococcal pili are composed of protofilaments exposing adhesive clusters of RrgA. *PLoS Pathog. 4*, No. e1000026.

(17) Hilleringmann, M., Ringler, P., Müller, S. A., De Angelis, G., Rappuoli, R., Ferlenghi, I., and Engel, A. (2009) Molecular architecture of *Streptococcus pneumoniae* TIGR4 pili. *EMBO J. 29*, 3921−3930.

(18) Fälker, S., Nelson, A. L., Morfeldt, E., Jonas, K., Hultenby, K., Ries, J., Melefors, O., Normark, S., and Henriques-Normark, B. (2008) Sortase-mediated assembly and surface topology of adhesive pneumococcal pili. *Mol. Microbiol. 70* (3), 595−607.

(19) Moschioni, M., Emolo, C., Biagini, M., Maccari, S., Pansegrau, W., Donati, C., Hilleringmann, M., Ferlenghi, I., Ruggiero, P., Antonia Sinisi, A., Pizza, M., Norais, N., Barocchi, M., and Masignani, V. (2010) The two variants of the *Streptococcus pneumoniae* pilus 1 RrgA adhesin retain the same function and elicit cross-protection *in vivo*. *Infect. Immun. 78*, 5033−5042.

(20) LeMieux, J., Hava, D. L., Basset, A., and Camilli, A. (2006) RrgA and RrgB are components of a multisubunit pilus encoded by the *Streptococcus pneumoniae rlrA* pathogenicity islet. *Infect. Immun. 74*, 2453−2456.

(21) LeMieux, J., Woody, S., and Camilli, A. (2008) Roles of the sortases of *Streptococcus pneumoniae* in assembly of the RlrA pilus. *J. Bacteriol. 190* (17), 6002−60013.

(22) El Mortaji, L., Terrasse, R., Dessen, A., Vernet, T., and Di Guilmi, A. M. (2010) Stability and assembly of pilus subunits of *Streptococcus pneumoniae*. *J. Biol. Chem. 285*, 12405−12415.

(23) Sung, C. K., Li, H., Claverys, J. P., and Morrison, D. A. (2001) An rpsL cassette, Janus, for gene replacement through negative selection in *Streptococcus pneumoniae*. *Appl. Environ. Microbiol. 67*, 5190−5196.

(24) Bricker, A. L., and Camilli, A. (1999) Transformation of a type 4 encapsulated strain of *Streptococcus pneumoniae*. *FEMS Microbiol. Lett. 172*, 131−135.

(25) Gentile, M. A., Melchiorre, S., Emolo, C., Moschioni, M., Gianfaldoni, C., Pancotto, L., Ferlenghi, I., Scarselli, M., Pansegrau, W., Veggi, D., Merola, M., Cantini, F., Ruggiero, P., Banci, L., and Masignani, V. (2011) Structural and functional characterization of the *Streptococcus pneumoniae* RrgB pilus backbone D1 domain. *J. Biol. Chem. 286*, 14588−14597.

(26) Izoré, T., Contreras-Martel, C., El-Mortaji, L., Manzano, C., Terrasse, R., Vernet, T., Di Guilmi, A. M., and Dessen, A. (2009) Structural basis of host cell recognition by the pilus adhesin from *Streptococcus pneumoniae*. *Structure 18*, 106−115.

(27) Quigley, B. R., Zähner, D., Hatkoff, M., Thanassi, D. G., and Scott, J. R. (2009) Linkage of T3 and Cpa pilins in the *Streptococcus pyogenes* M3 pilus. *Mol. Microbiol. 72* (6), 1379−1394.
(28) Smith, W. D., Pointon, J. A., Abbot, E., Kang, H. J., Baker, E. N., Hirst, B. H., Wilson, J. A., Banfield, M. J., and Kehoe, M. A. (2010) Roles of minor pilin subunits Spy0125 and Spy0130 in the serotype M1 *Streptococcus pyogenes* strain SF370. *J. Bacteriol. 192* (18), 4651−4659.
(29) Kang, H. J., Coulibaly, F., Clow, F., Proft, T., and Baker, E. N. (2007) Stabilizing isopeptide bonds revealed in Gram-positive bacterial pilus structure. *Science 318* (5856), 1625−1628.